

ORIGINAL RESEARCH

## Zoledronate can induce colorectal cancer microenvironment expressing BTN3A1 to stimulate effector $\gamma\delta$ T cells with antitumor activity

Maria Raffaella Zocchi<sup>a,\*</sup>, Delfina Costa<sup>b,\*</sup>, Roberta Venè<sup>b,\*</sup>, Francesca Tosetti<sup>b</sup>, Nicoletta Ferrari<sup>b</sup>, Simona Minghelli<sup>c</sup>, Roberto Benelli<sup>d</sup>, Stefano Scabini<sup>e</sup>, Emanuele Romairone<sup>e</sup>, Silvia Catellani<sup>f</sup>, Aldo Profumo<sup>g</sup>, and Alessandro Poggi<sup>b</sup>

<sup>a</sup>Division of Immunology, Transplants and Infectious Diseases, San Raffaele Scientific Institute, Milan, Italy; <sup>b</sup>Molecular Oncology and Angiogenesis, IRCCS AOU San Martino-IST, Genoa, Italy; <sup>c</sup>UOC Clinical and Experimental Immunology, IRCCS Istituto Giannina Gaslini, Genoa, Italy; <sup>d</sup>Immunology Unit, IRCCS AOU San Martino-IST, Genoa, Italy; <sup>e</sup>Oncological Surgery, IRCCS AOU San Martino-IST, Genoa, Italy; <sup>f</sup>Clinical Hematology, IRCCS AOU San Martino-IST, Genoa, Italy; <sup>g</sup>Biopolymers and Proteomics Unit IRCCS AOU San Martino-IST, Genoa, Italy

### ABSTRACT

Amino-bis-phosphonates (N-BPs) such as zoledronate (Zol) have been used in anticancer clinical trials due to their ability to upregulate pyrophosphate accumulation promoting antitumor  $V\gamma9V\delta2$  T cells. The butyrophilin 3A (BTN3A, CD277) family, mainly the BTN3A1 isoform, has emerged as an important structure contributing to  $V\gamma9V\delta2$  T cells stimulation. It has been demonstrated that the B30.2 domain of BTN3A1 can bind phosphoantigens (PAg) and drive the activation of  $V\gamma9V\delta2$  T cells through conformational changes of the extracellular domains. Moreover, BTN3A1 binding to the cytoskeleton, and its consequent membrane stabilization, is crucial to stimulate the PAg-induced tumor cell reactivity by human  $V\gamma9V\delta2$  T cells. Aim of this study was to investigate the relevance of BTN3A1 in N-BPs-induced antitumor response in colorectal cancer (CRC) and the cell types involved in the tumor microenvironment.

In this paper, we show that (i) CRC, exposed to Zol, stimulates the expansion of  $V\delta2$  T lymphocytes with effector memory phenotype and antitumor cytotoxic activity, besides sensitizing cancer cells to  $\gamma\delta$  T cell-mediated cytotoxicity; (ii) this effect is partially related to BTN3A1 expression and in particular with its cellular re-distribution in the membrane and cytoskeleton-associated fraction; (iii) BTN3A1 is detected in CRC at the tumor site, both on epithelial cells and on tumor-associated fibroblasts (TAF), close to areas infiltrated by  $V\delta2$  T lymphocytes; (iv) Zol is effective in stimulating antitumor effector  $V\delta2$  T cells from *ex vivo* CRC cell suspensions; and (v) both CRC cells and TAF can be primed by Zol to trigger  $V\delta2$  T cells.

### ARTICLE HISTORY

Received 16 August 2016  
Revised 22 December 2016  
Accepted 24 December 2016

### KEYWORDS

Amino-bis-phosphonates; butyrophilin; colorectal cancer; immunostimulation; phosphate antigens

## Introduction

Gammadelta ( $\gamma\delta$ ) T lymphocytes are involved in stress responses to injured, infected or transformed cells.<sup>1,2</sup> The most representative  $\gamma\delta$  T cell subset in the blood is the  $V\gamma9V\delta2$  (3–5% of circulating T lymphocytes), while the subset bearing the  $V\delta1$  chain is <1–2% and is mainly present in the mucosal-associated lymphoid tissue.<sup>1–3</sup>  $V\delta2$  T lymphocytes recognize unprocessed non-peptide molecules, including phosphoantigens (PAg) derived from the mevalonate pathway in mammalian cells, and via the 1-deoxy-D-xylulose-5-phosphate pathway, in bacterial cells.<sup>1–5</sup>  $\gamma\delta$  T cells also recognize NKG2D ligands (MICA, MICB and ULBPs), overexpressed at the cells surface by viral infections or tumor transformation.<sup>1–3</sup> Another activation signal can be delivered via Fc $\gamma$ RIIIa/CD16 that, upon interaction with the Fc of IgG, initiates the antibody-dependent cellular cytotoxicity to destroy opsonized cells or microorganisms.<sup>1–3</sup> After activation,  $\gamma\delta$  T cells proliferate, acquire cytotoxic ability and secrete a pattern of Th1 pro-inflammatory cytokines, such as IFN $\gamma$  and TNF $\alpha$ .<sup>1,2</sup> For this unconventional antigen recognition and multiple activation pathways,  $\gamma\delta$  T lymphocytes are antitumor effector

cells in several cancer types, including colorectal cancer (CRC), and potential suitable tools for anticancer therapy.<sup>3–8</sup>

Different drugs can be utilized to improve the mechanisms of  $\gamma\delta$  T cell activation:<sup>2,3,8</sup> in particular, synthetic pyrophosphate-containing compounds have been proposed for cancer immunotherapy on the basis of their ability to stimulate  $\gamma\delta$  T cells.<sup>9–12</sup> Moreover, aminobisphosphonates (N-BPs), in addition to their effect of inhibiting osteoclastic bone resorption,<sup>13</sup> lead to  $\gamma\delta$  T cell activation and proliferation, with a consequent increased number of  $\gamma\delta$  T cells in peripheral blood, displaying antitumor activity.<sup>14–18</sup> Indeed, N-BPs, such as zoledronate (Zol), are chemically stable analogs of inorganic pyrophosphate (IPP) that inhibit the mevalonate pathway and upregulate IPP accumulation, promoting antitumor  $V\gamma9V\delta2$  T cells *in vitro* and *in vivo*.<sup>15–20</sup> For this reason, different N-BPs have been used in anticancer clinical trials.<sup>21–24</sup>

In the last years, the butyrophilin 3A (BTN3A, CD277) family, structurally related to B7 co-stimulatory molecules, has emerged as important structure contributing to  $V\gamma9V\delta2$  T cell stimulation.<sup>25,26</sup> This family in humans is composed of three

**CONTACT** Alessandro Poggi, MSc, MD ✉ [alessandro.poggi@hsanmartino.it](mailto:alessandro.poggi@hsanmartino.it) Molecular Oncology and Angiogenesis, Department of Integrated Oncological Therapies, IRCCS AOU San Martino IST, Largo R. Benzi 10, 16132 Genoa, Italy.

Supplemental data for this article can be accessed on the publisher's website.

\*Co-first authors for equal contribution.

© 2017 Taylor & Francis Group, LLC

isoforms: BTN3A1, BTN3A2 and BTN3A3, characterized by two extracellular immunoglobulin domains, a transmembrane region and all, but BTN3A2, by a intracellular signaling domain, named B30.2.<sup>27,28</sup> It has been demonstrated that only the B30.2 domain of BTN3A1, thanks to a positively-charged pocket, can bind PAg and drive the activation of V $\gamma$ 9V $\delta$ 2 T cells through conformational changes of the extracellular domains.<sup>29-31</sup> Two recent reports describe the importance of BTN3A1 binding to the cytoskeleton, and its consequent membrane stabilization, to stimulate the PAg-induced tumor cell reactivity by human V $\gamma$ 9V $\delta$ 2 T cells;<sup>32</sup> PAg accumulation would also induce BTN3A1 conformational changes responsible for its recognition by V $\delta$ 2 T cells.<sup>33</sup>

In this paper, we show that (i) colon cancer cells, exposed to Zol, stimulate the expansion of V $\delta$ 2 T cells with effector memory (EM) phenotype and cytotoxic activity; (ii) this effect is partially related to BTN3A1 expression and cellular re-distribution; (iii) BTN3A1 is detected in CRC at the tumor site, both on epithelial and on stromal cells, close to areas infiltrated by V $\delta$ 2 T lymphocytes; (iv) Zol is effective in stimulating antitumor effector V $\delta$ 2 T cells from *ex-vivo* CRC cell suspensions; and (v) both CRC cells and tumor-associated fibroblasts (TAF) can be primed by Zol to trigger V $\delta$ 2 T cells.

## Results

### CRC exposed to Zol stimulate the expansion of V $\delta$ 2 T cells with antitumor cytotoxic activity

Fourteen different established CRC cell lines (Colo205, Colo741, Colo320, SW620, HCT15, HCT116, DLD1, WiDr, LoVo, LS180, HT29, CaCo2, SW48 and SW480) were co-cultured with peripheral blood T cells from healthy donors, at the T: CRC ratio of 10:1, in the presence or absence of 5  $\mu$ M Zol and IL2. As shown in Fig. 1, many of these CRC cell lines (LS180, LoVo, WiDr, Colo741, Colo320 and to a lesser extent SW620, HT29, DLD1 and Colo205), when exposed to Zol, were able to induce the expansion of  $\gamma\delta$  T lymphocytes, after 20 d of culture (Figs. 1A and 1C, 4 representative CRC cell lines; Fig. 1B, all the cell lines tested, mean  $\pm$  SD from six experiments with six different T cell donors for each cell line). Indeed, the percentage of  $\gamma\delta$  T lymphocytes raised from less than 5% in the starting T cell populations (range 2–5%, not shown), up to 80% in the co-cultures with Zol-treated CRC (Fig. 1A lower panels vs. IL2 alone in upper panels; Fig. 1B dark gray columns), values superimposable to those obtained using monocytes<sup>16</sup> exposed to Zol (Fig. 1B). No expansion of  $\gamma\delta$  T cells was detected in the co-cultures set up in the absence of Zol (Fig. 1A upper panels and Fig. 1B white columns). Zol added to purified T cells alone did not exert any stimulating effect (Fig. 1A, lower left panel, one representative experiment).

As it has been reported that several tumor cell lines require higher doses of Zol to exert their stimulating activity of  $\gamma\delta$  T cells,<sup>34</sup> three low-stimulating (SW620, HCT15, DLD1) and one stimulating (LS180) CRC cell lines were pre-treated (4 h) with high doses (100  $\mu$ M and 50  $\mu$ M) of Zol, washed and co-cultured with purified T cells as above. As shown in Fig. 1C, high doses of Zol were effective on LS180 cell line, while the other

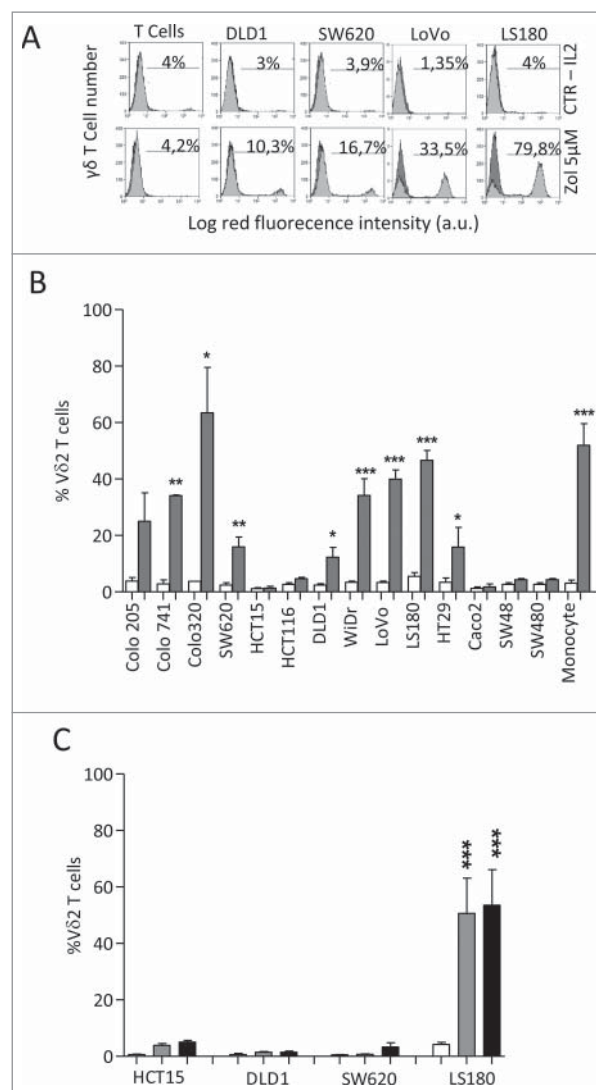


**Figure 1.** V $\delta$ 2 T cell expansion upon co-culture with CRC exposed to Zol. The CRC cell lines HT29, HCT15, HCT116, SW48, SW620, SW480, Colo741, Colo205, Colo320, CaCo2, LS180, WiDr, LoVo and DLD1 were co-cultured for 20 d with peripheral blood T cells from healthy donors, at the T: CRC ratio of 10:1, with 5  $\mu$ M Zol and IL2 or IL2 alone. (A) percentage of V $\delta$ 2 T lymphocytes among one representative T cell population cultured alone (left histograms) and after co-culture with CRC (other panels, four representative CRC cell lines) with Zol (lower row) or IL2 alone (upper row) evaluated with the anti-V $\delta$ 2 mAb and FACS analysis. Data are represented as percentage of V $\delta$ 2 T cells (light gray histograms) reported in each quadrant. (B) percentage of V $\delta$ 2 T lymphocytes after 20 d of co-culture with the indicated CRC cell lines with Zol (gray columns) or IL2 alone (white columns). Data are the mean  $\pm$  SD from six experiments for each cell line. \* $p$  < 0.05, \*\* $p$  < 0.01, \*\*\* $p$  < 0.001 vs. co-cultures without Zol. (C) SW620, HCT15, DLD1 and LS180 CRC cell lines were pre-treated (4 h) with high doses (100  $\mu$ M, black bars, or 50  $\mu$ M, gray bars) of Zol, washed and co-cultured with purified T cells as above, and evaluated for the percentage of V $\delta$ 2 T lymphocytes after 20 d of co-culture. Mean  $\pm$  SD from six experiments with T cells of six different donors. \*\*\* $p$  < 0.001 vs. co-cultures without Zol.

cell lines did not acquire the ability to stimulate  $\gamma\delta$  T cell growth even at the highest dose of Zol.

We chose the LS180 cell line as an example of stimulating CRC cells, to analyze the phenotype of the  $\gamma\delta$  T cell populations obtained after 20 d of culture. In particular, we focused on the distinction of naive (N), bearing CD27 and CD45RA molecules, central memory (CM), showing only CD27, EM that are double negative, and terminal-differentiated memory cells (TEMRA) that are surface positive CD45RA.<sup>35,36</sup> We found that upon Zol

treatment, LS180 cells could drive the expansion of  $\gamma\delta$ T cells showing the characteristics of EM T lymphocytes (i.e., absence of CD27 and CD45RA) (Fig. 2A, two representative experiments; Fig. 2B mean of eight experiments). Of note, this  $\gamma\delta$  T cell population exerted a cytotoxic activity against the stimulating LS180 cell line (Fig. 2C, left panel white columns) and against two other cell lines (Fig. 2C white columns: HCT15, central panel; DLD1, right panel); the cytolytic effect was enhanced by exposing the CRC cell lines used as targets to Zol (Fig. 2C, dark gray columns). Similar results, were obtained with WiDr, Colo320 and LoVo stimulating cell lines in two experiments for each cell line (not shown). These data indicate that Zol added to CRC cells, besides determining their sensitization to cytotoxicity exerted by activated  $\gamma\delta$  T cells, induces the expansion of EM  $\gamma\delta$  T lymphocytes able to kill both the stimulating tumor cells and other cancer cell lines.

### BTN3A1 contributes to zoledronate effect in CRC cell lines

We then investigated the heterogeneity of the stimulating ability displayed by the various CRC cell lines. As BTN3A1 is a molecule essential for the recognition of phosphate antigens by  $\gamma\delta$  T lymphocytes,<sup>25-31</sup> we first analyzed BTN3A1 protein by immunofluorescence and by western blot with the anti-CD277 mAb recognizing the immunoglobulin-like extracellular domain of BTN3A1, or with a rabbit polyclonal anti-BTN3A1 antiserum recognizing the C-terminal domain of the

molecule. We found no significant difference in the surface expression of CD277, evaluated by cytofluorimetric analysis; however, the reactivity of this antibody in immunofluorescence is very low, also on healthy monocytes (not shown). In western blot, the same mAb could recognize the major reported bands for BTN3A1 (Fig. 3A, 57 kDa and 37 kDa) in most CRC cell lines, with the exception of CaCo2 cells; the 57 kDa band was identified also by the anti-BTN3A1 antiserum in the majority of cell lines and the 37 kDa band was evident in CaCo2 and HT29 cells (Fig. 3A). These data would indicate that the efficiency in Zol stimulating effect is not directly related to the amount of BTN3A1 expressed; indeed, some stimulating cells showed low levels of BTN3A1 in immunoblotting (LoVo), whereas in some low stimulators a strong reactivity was detected (HCT15, HCT116) (Fig. 3). Thus, we asked whether the different distribution of BTN3A1, in particular its membrane localization or cytoskeletal association, was responsible for the activity of the molecule, as recently reported.<sup>32,33</sup> We found that in DLD1 (a low-stimulating CRC cell line) a considerable amount of protein is detected in the cytosolic fraction (Fig. 3B, left blot, Cyt), probably containing also small vesicles not pelleted at low speed after nuclei isolation, while in the stimulating LS180 cell line BTN3A1 is mainly present in the membrane-enriched fraction (Fig. 3B, right blot, M). Upon Zol treatment, BTN3A1 is also detectable in the cytoskeleton-enriched fraction (that contains detergent-resistant cell-membrane fragments tightly linked to the

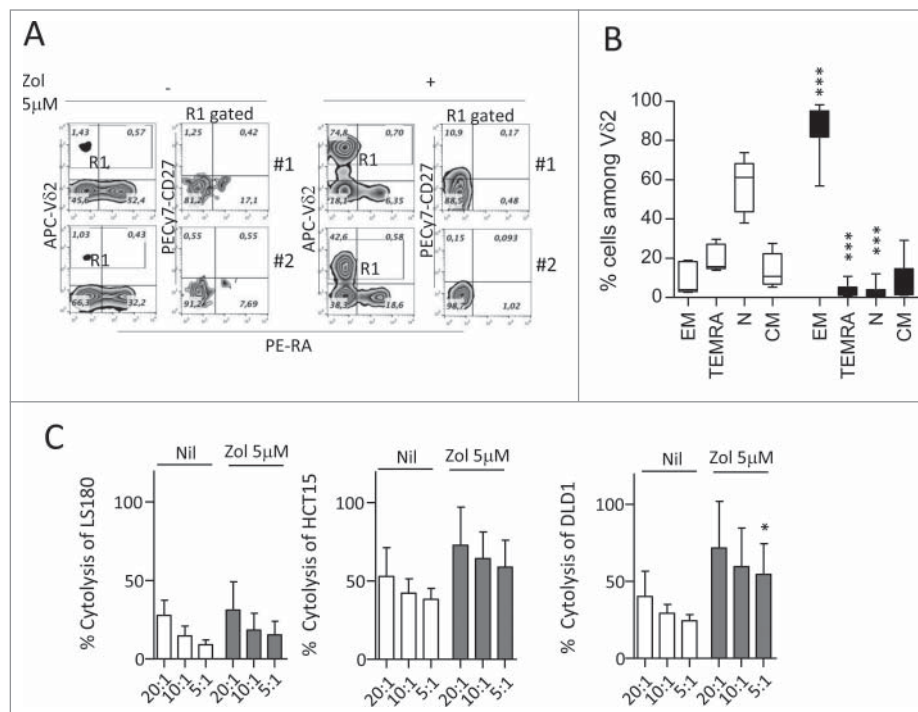


**Figure 2.** Expansion of effector memory antitumor  $\delta$ 2 T cell lymphocytes upon co-culture with Zol-treated LS180 CRC cell line. Panels A and B: Peripheral blood T lymphocytes were co-cultured for 20 d with LS180 CRC cell line, in the absence or presence of Zol ( $5 \mu\text{M}$ ) and IL2. (A) Representative phenotype of  $\delta$ 2 T cells from two donors (donor 1, upper plots, donor 2, lower plots), co-cultured with LS180 and IL2 alone or with Zol-treated LS180, stained with APC-anti  $\delta$ 2, PE-anti-CD27 and PE-Cy7-anti-CD45RA. (B) Results expressed as percentage of effector memory (EM,  $\text{CD45RA}^- \text{CD27}^-$ ) T cells, terminal-differentiated effector memory (TEMRA,  $\text{CD45RA}^+ \text{CD27}^-$ ) T cells, naive (N,  $\text{CD45RA}^+ \text{CD27}^+$ ) T cells or central memory (CM,  $\text{CD45RA}^- \text{CD27}^+$ ) among  $\delta$ 2 T lymphocytes immediately after separation (white bars) or on day 20 of co-culture with LS180 cells (black bars). Mean  $\pm$  SD from eight experiments.  $***p < 0.001$  versus T lymphocytes after separation (white bars). (C):  $\delta$ 2 T cells derived from co-cultures with Zol-treated LS180 CRC cells were tested in a  $^51\text{Cr}$  release assay against untreated (white bars) or Zol-treated ( $5 \mu\text{M}$  for 24 h, gray bars) LS180 (left histogram) HCT15 (central histogram) or DLD1 (right histogram) cell lines at the E:T ratio of 20:1, 10:1 and 5:1. Results are expressed as percentage specific lysis, calculated as described in Materials and Methods, the mean  $\pm$  SD from three experiments is shown.  $*p < 0.05$  vs. Nil.

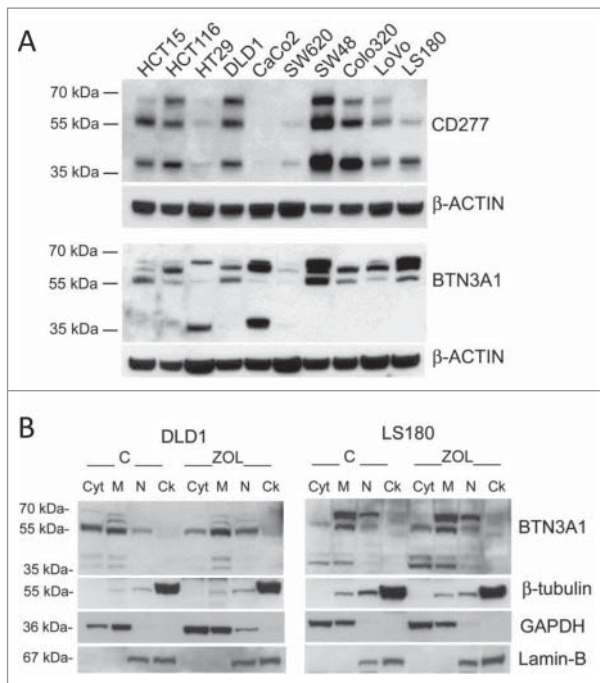


**Figure 3.** BTN3A1 expression and subcellular localization in CRC cell lines. (A) BTN3A1 was evaluated in CRC cell lines by western blot. Immunoblot of cell lysates obtained from the indicated CRC cell lines as described in Materials and Methods, was probed with the anti-CD277 mAb (upper blot), or with a rabbit polyclonal anti-BTN3A1 antiserum (lower blot).  $\beta$ -actin was used as a loading control. (B) BTN3A1 localization in subcellular fractions (Cyt: cytosolic fraction, M: membrane-enriched fraction, N: nuclear fraction, Ck: cytoskeleton-enriched fraction) obtained with the Qproteome cell compartment kit from untreated or Zol-treated ( $10 \mu\text{M}$  for 24 h) DLD1 (left panel) or LS180 (right panel), as indicated. In each panel:  $\beta$ -tubulin as marker of Ck fractions, GAPDH for the Cyt/M fractions, lamin B for the N fraction.

cytoskeletal proteins, so that they are insoluble) (Fig. 3B, Ck), in agreement with recent reports.<sup>33</sup> In addition, it has to be noted that BTNL2, known to downregulate the effect of BTN3A1,<sup>27,37</sup> was expressed at very low levels in stimulating cell lines, in particular Colo320, LS180, LoVo, Colo205 and WiDr, at variance with low-stimulating cell lines (Fig. S1).

In further experiments, we tried to potentiate Zol effect in low-stimulating CRC cell lines, by enhancing BTN3A1 expression. To this aim, SW620 or DLD1 cell lines were transfected with a BTN3A1-containing plasmid and used both as stimulators of V $\delta$ 2 T cell growth, and as target cells, upon Zol exposure. Transfected cells were collected at the different time points, irradiated to avoid the overgrowth of untransfected cells, and BTN3A1 expression was evaluated by western blot on day 2, 4 or 5 and 7 after transfection. As shown in Fig. 4, transfection was efficient and BTN3A1 overexpression lasted up to one week (Fig. 4A: SW620 and Fig. 4B: DLD1) and it was not altered by irradiation. Also, the ability to stimulate V $\delta$ 2 T cell expansion in the presence of Zol was increased in BTN3A1 transfected, compared with wild type (WT), SW620 and DLD1 cells, although the difference was not significant, due to the variable response of T lymphocytes isolated by three different donors (Fig. 4C). Likewise, SW620 and DLD1 transfected cells acquired a higher sensitivity to V $\delta$ 2 T cell killing upon exposure to Zol (Fig. 4D).

### Differential IPP production by CRC cell lines upon Zol treatment

To further investigate the heterogeneity in the stimulating ability displayed by the different CRC cell lines, we measured the IPP production in response to Zol, either as continuous treatment with  $5 \mu\text{M}$  for 24 h, or as pulse treatment of  $50 \mu\text{M}$  and  $100 \mu\text{M}$  for 4 h, by high-pressure liquid chromatography (HPLC) negative ion electrospray ionization time of flight mass spectrometry (TOF-MS), in DLD1, SW620, HCT15 (non-stimulating), LS180 and Colo320 (stimulating) cell lines.<sup>38</sup> As shown in Fig. 5, LS180 cell line stimulated with Zol  $5 \mu\text{M}$  for 24 h (panel Aa) produced about 3-fold or 7-fold IPP than DLD1 (panel Ba) or SW620 (panel Ca) cells, respectively. In addition, the response of LS180 (Fig. 5Ac) or Colo320 (not shown) and, to a lesser extent, of DLD1 (Fig. 5Bc) cell lines was more evident when treated with a pulse of Zol at high concentrations ( $100 \mu\text{M}$ ). At variance, SW620 (Fig. 5Cc) and HCT15 (not shown) were not able to enhance IPP production, even when exposed to high Zol concentrations.

### Zoledronate is effective in stimulating V $\delta$ 2 effector T cells from ex-vivo CRC cell suspensions

To verify the possible effect of Zol in the tumor microenvironment, we isolated cell suspensions from different CRC specimens and performed cell cultures in the presence or absence of Zol ( $5 \mu\text{M}$  on day 0, IL2 added on day 1). As shown by immunofluorescence analysis (Fig. 6A), the starting cell population (FACS analysis in open gate on viable cells on the basis of forward and side scatter, FSC and SSC) was composed of T lymphocytes (CD3<sup>+</sup>, about 25%), a small fraction of which (< 5%) bearing the V $\delta$ 2 T cell receptor, epithelial cells (EPCAM<sup>+</sup>, from 15 to 55%), 2–5% of monocytes (CD14<sup>+</sup>) and 5–10% of stromal cells (CD105<sup>+</sup>, as a marker of mesenchymal cells, Fig. 6A), possibly TAF. After 20 d, in Zol-treated cultures a 10- to 2-fold increase in V $\delta$ 2 T lymphocytes was observed in most cases (Fig. 6B, left panels: the best experiment, central and right histograms: mean  $\pm$  SEM of eight CRC cultures). When tested in re-directed killing assay, the V $\delta$ 2-enriched T cell cultures could be activated by the anti-CD3 and anti-V $\delta$ 2 mAbs, but not by anti-CD8<sup>+</sup> or unrelated mAbs (Fig. 6C); moreover, these cell populations showed a remarkable cytolytic activity against CRC cell lines (Fig. 6D, left and right panels). This data indicate that Zol added to *ex-vivo* tumor-derived cell suspensions, containing epithelial cells, lymphocytes, TAF and monocytes, is effective in inducing the expansion of infiltrating V $\delta$ 2 T cells with potential antitumor activity.

Along this line, we found that TAF isolated from four CRC specimens, characterized as CD105<sup>+</sup> (as marker of mesenchymal cells) and FAP<sup>+</sup> (not shown), express BTN3A1 (Fig. 7A; note the presence of vimentin and absence of cytokeratin in TAF lysate). When exposed to Zol, TAF were able to induce V $\delta$ 2 T cell expansion (Fig. 7B, left panels: one representative case of TAF cultured with T lymphocytes isolated from two healthy donors; Fig. 7C, left histograms, black columns: mean  $\pm$  SEM of four CRC-derived TAF:T co-cultures). Again, this V $\delta$ 2 T cell population was mainly EM (Fig. 7C, right histograms, black columns) and could be activated in re-directed killing

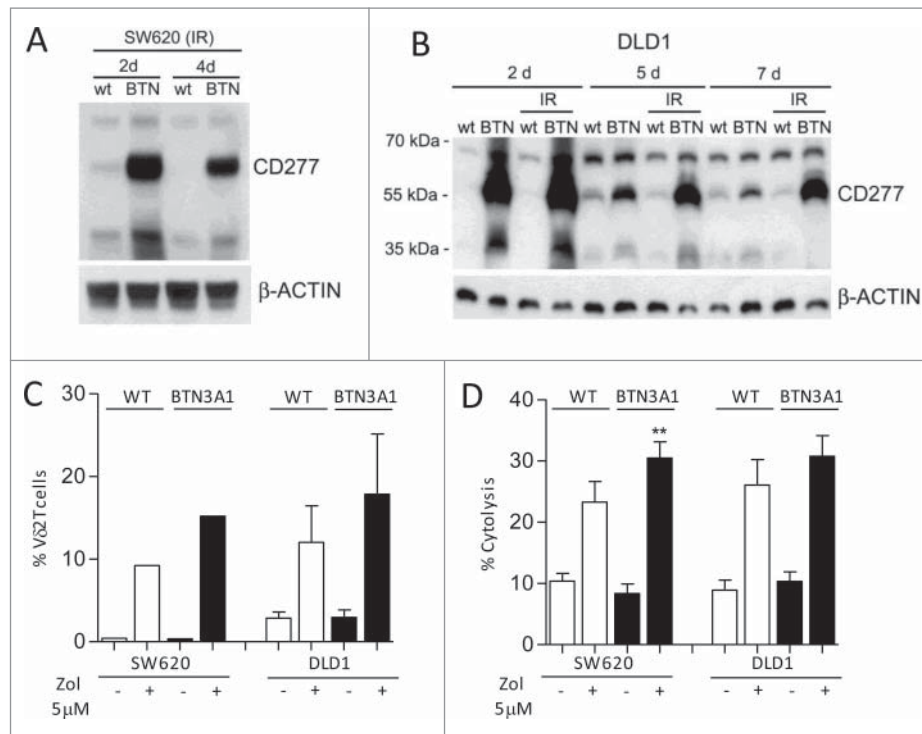


**Figure 4.** Enhancement of BTN3A1 expression and expansion of antitumor V $\delta$ 2 T cells. SW620 (A, C, D) or DLD1 (B, C, D) cells were transfected with BTN3A1-containing plasmid and irradiated to avoid the overgrowth of untransfected cells; expression was evaluated on day 2, 5 and 7 by western blot using the anti-CD277 (A, B). (C) Wild type (WT, white columns) or BTN3A1-transfected (black columns) SW620 or DLD1 cells, untreated or treated with Zol (5  $\mu$ M), as indicated were co-cultured with purified T lymphocytes: the percentage of V $\delta$ 2 T cells was evaluated by immunofluorescence with the specific anti-V $\delta$ 2 mAb and FACS analysis after 20 d of culture; results are expressed as percentage V $\delta$ 2 T lymphocytes and are the mean  $\pm$  SEM from three transfection experiments with six different T cell donors for DLD1; one representative experiment with two T cell donors for SW620. (D) WT (white columns) or BTN3A1-transfected (black columns) SW620 or DLD1 cells, untreated or treated with Zol (5  $\mu$ M) as indicated, were used as targets in a 4 h  $^{51}$ Cr release assay using as effectors IL-2-activated peripheral blood V $\delta$ 2 T cells at the E:T ratio of 10:1. Results are expressed as percentage specific lysis, calculated as described in Materials and Methods, and are the mean  $\pm$  SEM from three experiments. \*\* $p$  < 0.01 vs. Zol-treated WT SW620.

assay by the anti-T cell receptor V $\delta$ 2 mAb and by the anti-CD3 mAb, but not by anti-CD8 $^{+}$  or an unrelated, isotype-matched mAb (Fig. 7D, black columns). Also, effector  $\gamma\delta$  T lymphocytes were able to kill CRC cells with higher efficiency, and lower E:T ratios, when target cells were exposed to Zol (Fig. 7E, left histograms, black vs. white columns). Also, we found that two epithelial cell lines (CRC15-045 and CRC13-011) obtained as primary cultures from two CRC, expressed BTN3A1 (Fig. 7A shows CRC15-045; note the presence of cytokeratin and absence of vimentin in the cell lysate). Once treated with Zol, both CRC15-045 and CRC13-011 cells were able to stimulate the expansion of EM V $\delta$ 2 T lymphocytes (Fig. 7B, right panels: two representative experiments with CRC15-045 and T lymphocytes isolated from two healthy donors; Fig. 7C, left and right histograms, gray columns: mean  $\pm$  SEM,  $n$  = 2 epithelial cell lines with two T cell donors). This V $\delta$ 2 T cell population could be activated by anti-V $\delta$ 2 (BB3) and anti-CD3 (UCHT1) mAb (Fig. 7D, gray columns: mean  $\pm$  SEM,  $n$  = 2 epithelial cell lines with two T cell donors) and kill the CRC cell line CaCo2 (Fig. 7E, right histograms, gray columns) and HCT15 (not shown). Thus, in the presence of Zol, both TAF- and tissue-derived CRC can induce the expansion of V $\delta$ 2 effector T cells with antitumor cytotoxic activity. It is of note that in TAF BTN3A1 is mainly localized in the membrane- and cytoskeleton-enriched fractions, and this is more evident upon Zol exposure (Fig. 7F, M vs. Ck).

Finally, V $\delta$ 2 effector T cells showing antitumor activity can be derived from tumor cell suspensions also using monocytes, isolated from peripheral blood of healthy donors (we could not obtain enough monocytes from CRC cell suspensions), in the presence of Zol (Fig. S2A: two representative experiments; Fig. S2B: mean  $\pm$  SD of five monocyte: CRC cultures, left histograms: percentage of V $\delta$ 2 T cells; right histograms: fold increase vs. the beginning of culture). The cytolytic activity was stimulated by anti-V $\delta$ 2 and anti-CD3 mAbs as re-directed killing assay (Fig. S2C) or was detected using CRC cells (Fig. S2D, HCT15: left histogram, CaCo2: right histogram). All these data would indicate that Zol can enable different cell types present in the CRC microenvironment (cancer cells, TAF and monocytes) to induce the expansion of antitumor effector  $\gamma\delta$  T lymphocytes.

To confirm that Zol can work *in vivo*, we checked the expression of BTN3A1 at the tumor site. As shown in Fig. 8, BTN3A1 could be detected by PCR in CRC specimens (Fig. 8A, 10 CRC examined), and by western blot as protein in cell lysates obtained from the same CRC samples (Fig. 8B, BTN3A1 detected using either anti-CD277 mAb or anti-BTN3A1 antiserum). Immunohistochemistry (Fig. 8C, two representative cases out of 10 CRC) showed that BTN3A1 can be detected on either epithelial cells or TAF (transglutaminase, TGII or vimentin positive) in CRC, close to areas infiltrated by V $\delta$ 2 T lymphocytes (recognized by the anti-V $\delta$ 2 mAb BB3).

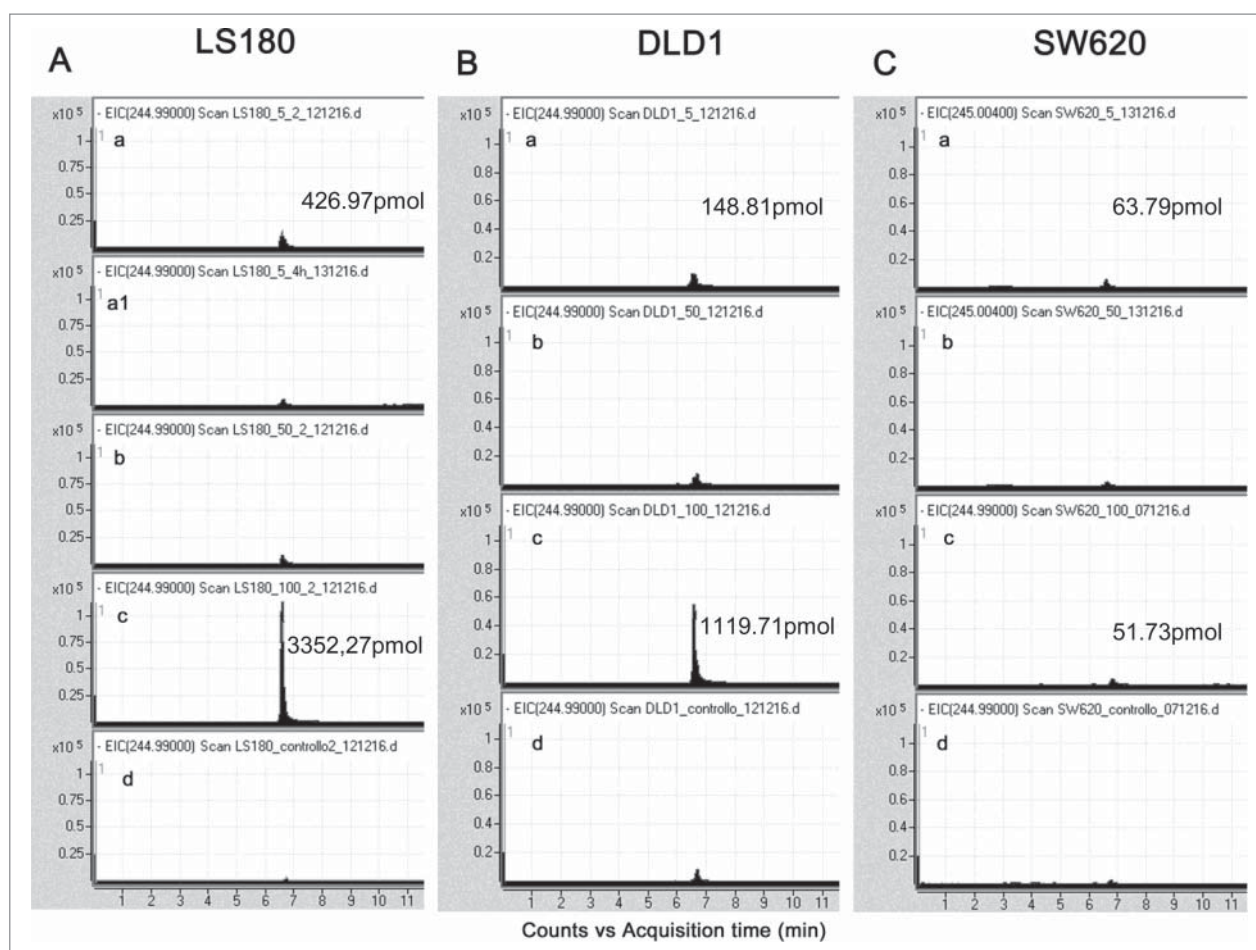


**Figure 5.** Measurement of IPP produced by SW620, DLD1 or LS180 CRC cell lines upon exposure to Zol. Acetonitrile extracts from LS180 (A), DLD1 (B) and SW620 cells (C) untreated (d) or treated with 5 μM Zol for 24 h (a), or 50 μM (b) and 100 μM (c) Zol for 4 h and maintained in culture for additional 20 h, were analyzed by HPLC/TOF-MS. The relative abundance of the extracted ion current (EIC) (m/z 244.99 [M-H]<sup>-</sup>) for IPP/DMAPP (3,3-dimethylallyl pyrophosphate) is shown. LS180 cells were also exposed to 5 μM Zol for 4 h (Aa, a1), to test early effects of low-dose Zol, giving no appreciable increase of IPP over controls. Quantification of IPP produced upon exposure to either 5 μM Zol for 24 h (Aa, Ba, Ca) or 100 μM Zol for 4 h (Ac, Bc, Cc) in the indicated CRC cell lines. Data are shown as IPP pmol/mg of total pmol extracted by ACN/total protein content in cell lysates after ACN extraction.

## Discussion

There is general agreement on the role of  $\gamma\delta$  T lymphocytes-infiltrating solid tumors, including CRC, in the anticancer surveillance,<sup>3-5,9,11</sup> so that treatments focused on  $\gamma\delta$  T cell-mediated immune responses are now considered as an attractive and promising therapeutic approach in oncology.<sup>6-8,39,40</sup> Stimulation of  $\gamma\delta$  T lymphocytes with PAg,<sup>3,6-11</sup> through the engagement of the BTN3A1 molecule,<sup>25-31</sup> leads to the generation of an efficient antitumor immune response. In particular, N-PBs that induce IPP accumulation, have been used in different clinical trials.<sup>21-24</sup>

In this paper, we show that (i) the N-BP Zol, besides sensitizing CRC cells to  $\gamma\delta$  T cell-mediated cytotoxicity, stimulates the expansion of V $\delta$ 2 T cells with EM phenotype and antitumor cytotoxic activity; (ii) this effect is partially related to BTN3A1 expression and in particular by its cellular re-distribution; (iii) BTN3A1 is detected at the tumor site, both on epithelial and stromal cells, in the areas infiltrated by V $\delta$ 2 T lymphocytes; (iv) Zol is effective in stimulating antitumor effector V $\delta$ 2 T cells from *ex-vivo* CRC cell suspensions; and (v) both CRC cells and TAF can be primed by Zol to trigger V $\delta$ 2 T cells.

First, we found that different CRC cell lines exposed to Zol as a source of IPP, could successfully promote the expansion of  $\gamma\delta$  T lymphocytes able to kill both the stimulating tumor cells and other CRC cell lines. The phenotype of such lymphocyte population, that was mostly naive (co-expression of CD45RA and CD27) at the beginning of the co-culture, was that of EM cells, based on the lack of CD45RA and CD27 expression.<sup>35,36</sup> Furthermore, Zol could sensitize CRC cell lines, including those that poorly triggered  $\gamma\delta$  T cell growth, to become targets for the cytotoxic effect exerted by activated  $\gamma\delta$  T lymphocytes. Given the heterogeneity of the stimulating ability displayed by the various CRC cell lines, we asked whether this was due to a different sensitivity of farnesyl diphosphate synthase to Zol, as reported.<sup>34</sup> However, non-stimulating CRC cell lines were unable to trigger efficiently  $\gamma\delta$  T cell expansion, even when pre-treated with high doses of Zol; furthermore, IPP production in response to Zol, was lower in the three non-stimulating cell lines tested and they did not enhance IPP production in response to high doses of Zol, with the exception of DLD1. Thus, we further investigated any possible difference in the expression of proteins of the butyrophilin family, mainly BTN3A1 that is an essential molecule for

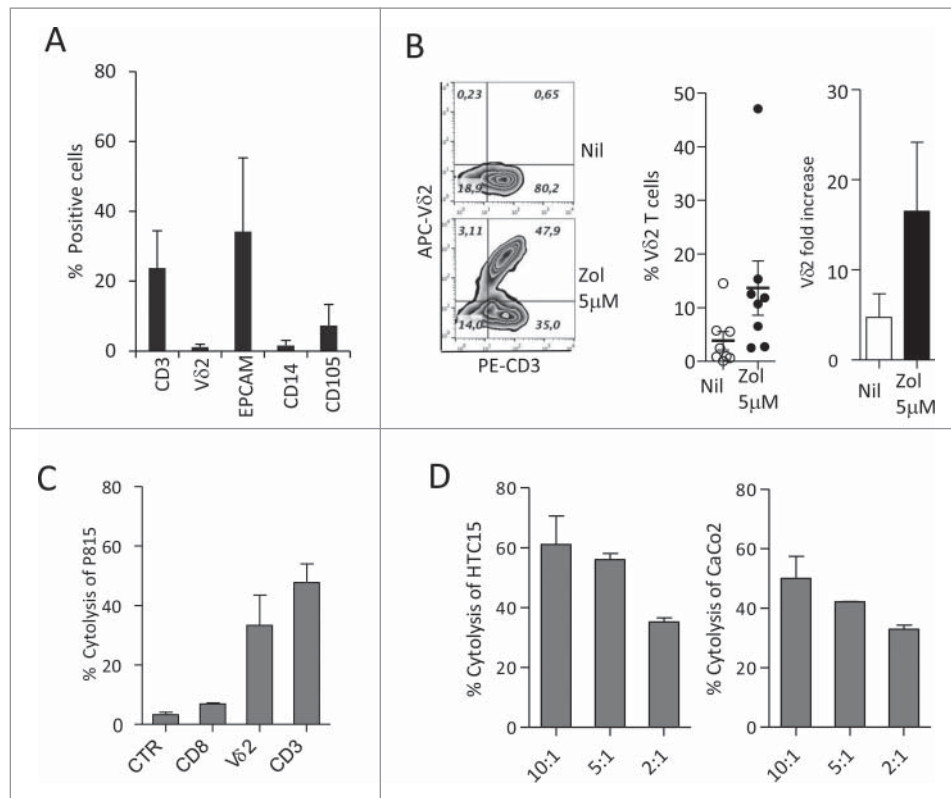


**Figure 6.** Differentiation of Vδ2 T cells from *ex-vivo* CRC cell suspensions. (A) Cell suspensions from CRC were stained with specific anti-CD3, anti-Vδ2, anti-EPCAM, anti-CD14 and anti-CD105 mAbs followed by aAPC-conjugated anti-isotype antiserum and analyzed by flow cytometry. Percentages of positive cells were calculated and results expressed as mean ± SD (n = 10). (B) CRC cell suspensions were cultured in the presence or absence of Zol (5 μM) and IL2 for 20 d, double stained with the specific PE-anti-CD3 and APC-antiVδ2 mAbs and the percentage of positive cells was calculated. Left plots: one representative experiment out of eight. Central histogram: percentage of Vδ2 T cells obtained from CRC cultures without (white) or with Zol (5 μM, black); mean ± SEM of eight experiments. Right histogram: results analyzed as fold increase (percentage of Vδ2 T cells on day 20 vs. day 0, white bar IL2 alone, black bar 5 μM Zol). Mean ± SEM (n = 8). (C and D) Vδ2 T cells obtained from 20 d of CRC cultures, with Zol, were used in re-directed killing assay against the P815 cell line in the presence of the anti-CD8, anti-Vδ2, anti-CD3 mAbs or an unrelated mAb matched for the isotype (CTR) (C) at the E:T ratio of 5:1, or in a 4 h <sup>51</sup>Cr release cytolytic assay against the HCT15 or CaCo2 cell lines (D, left and right histograms) at the E:T ratio of 10:1, 5:1 and 2:1. One representative experiment of three is shown. Mean ± SEM of sample duplicate.

the recognition of PAg by γδ T lymphocytes, due to its B30.2-binding domain.<sup>25-31</sup>

The amount of BTN3A1 mRNA evaluated by Q-RT-PCR analysis is heterogeneous in stimulating and in low-stimulating CRC cell lines (not shown); the expression of the protein assayed with the anti-CD277 mAb, recognizing the immunoglobulin-like extracellular domain, was not clearly detectable in the CRC cell lines, regardless of their ability to promote γδ T cell expansion. When BTN3A1 expression was assayed with an anti-BTN3A1 antiserum recognizing the cytoplasmic tail of the molecule, at least one of the two major reported bands for BTN3A1<sup>7,32,33</sup> was detected in most CRC cell lines, regardless of their stimulating efficiency. This could explain the finding that also low-stimulating CRC, once treated with Zol, can be killed by γδ T lymphocytes. On the other hand, overexpression of BTN3A1 obtained by transfection in two CRC cell lines (SW620 and DLD1) could only partially enhance their stimulating activity or their sensitivity to γδ T cell killing upon Zol treatment. It has to be noted that no significant differences in the transcription of the other members of BTN3A family, i.e., BTN3A2 and BTN3A3, was found in the different CRC cell lines (not shown); however, BTNL2, known to downregulate the effect of BTN3A1,<sup>37</sup> was poorly expressed in most of the stimulating cell lines.

Based on these data, the role of BTN3A1 molecule does not appear to be directly related to the amount of protein expressed; rather, the different distribution of BTN3A1, in particular its cell membrane localization or cytoskeletal association, may be responsible for the activity of the molecule.<sup>32</sup> It has been recently reported that a PAg-induced conformational change in BTN3A1 leads to its recognition by Vγ9Vδ2 TCR.<sup>33</sup> In agreement with this finding, we found that Zol treatment induces a re-distribution of BTN3A1 in TAF and, to a lesser extent in CRC cells, increasing its binding to the cell membrane and to the cytoskeleton, thus explaining the efficiency in stimulating Vδ2 T cell expansion and effector function. Nevertheless, CRC cells should also display a functional farnesyl diphosphate synthase to produce IPP and deliver an efficient activating signal to γδ T lymphocytes.

An interesting observation is that Zol added to *ex-vivo* tumor-derived cell suspensions, containing epithelial cells, lymphocytes, TAF and monocytes, is effective in inducing the growth of γδ T cells showing cytolytic activity against CRC target cells. Thus, whatever the mechanism of BTN3A1 responsible for Zol-induced IPP accumulation, using this drug it is possible to induce the expansion of infiltrating γδ T cells with potential antitumor activity. Along this line, in the presence of

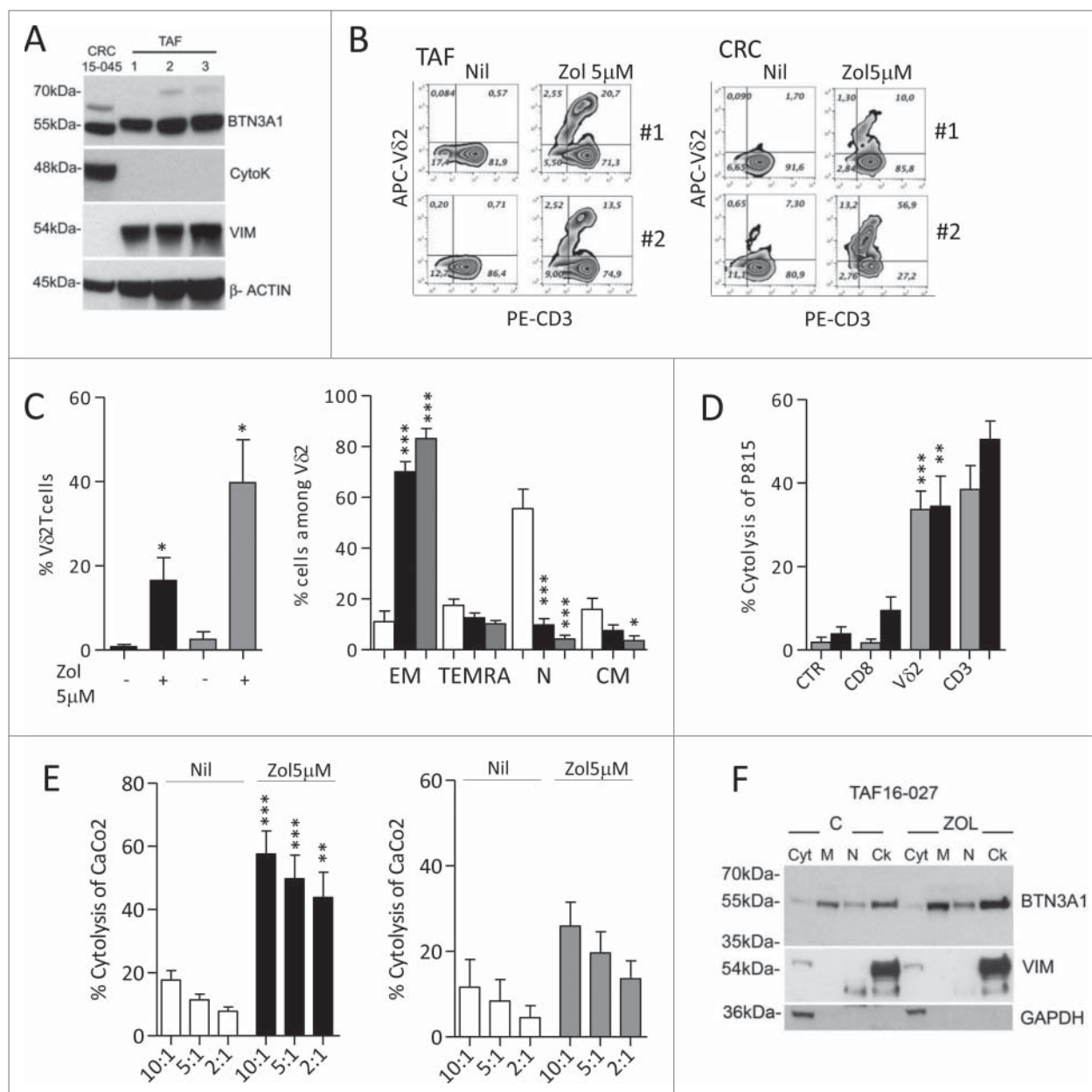


**Figure 7.** Differentiation of effector memory antitumor  $V\delta 2$  T cells induced by tumor-associated fibroblast (TAF) and tumor-derived CRC primary cultures. (A) Immunoblot of cell lysates obtained from three TAF (TAF16–020, TAF16–027 and TAF16–030) or the CRC15–045 epithelial cell primary culture, with polyclonal anti-BTN3A1 antiserum, anti-cytokeratin and anti-vimentin mAbs.  $\beta$ -actin is shown as a loading control. (B) Peripheral blood T lymphocytes were co-cultured with TAF (left plots: T cells from donor 1 and donor 2 upon culture on TAF16–020) or CRC15–045 epithelial cell culture (right plots, T cells from donor 1 and donor 2), pre-treated with Zol ( $5\ \mu\text{M}$ ) or not (Nil) for 20 d and double stained with PE-anti-CD3 and APC-anti- $V\delta 2$ mAbs. The percentage of  $V\delta 2$  T cells is reported in the upper right quadrant of each plot. (C) Left histogram: percentage of  $V\delta 2$  T cells obtained from 20 d of co-culture with untreated or Zol-treated TAF (black) or untreated or Zol-treated CRC15–045 and CRC13–011 epithelial cells (gray). Mean  $\pm$  SEM ( $n = 8$  experiments performed with two T lymphocyte donors and four TAF;  $n = 4$  experiments with two T lymphocyte donors and the two CRC epithelial cells). Right histograms: percentage of effector memory (EM,  $\text{CD45RA}^+\text{CD27}^-$ ), terminal-differentiated effector memory (TEMRA,  $\text{CD45RA}^+\text{CD27}^-$ ), naive (N,  $\text{CD45RA}^+\text{CD27}^+$ ) or central memory (CM,  $\text{CD45RA}^-\text{CD27}^+$ ) cells among  $V\delta 2$  cells from T lymphocytes immediately after separation (white bars) or on day 20 of co-culture with Zol-treated TAF cells (black bars) or CRC15–045 and CRC13–011 epithelial cells (gray bars). Mean  $\pm$  SEM as above.  $****p < 0.0001$  or  $**p < 0.01$  or  $*p < 0.05$  vs. T lymphocytes after separation (white bars). (D, E)  $V\delta 2$  T cells obtained from T lymphocytes after 20 d of co-culture with Zol-treated TAF or CRC epithelial cells were used in re-directed killing assay against the P815 cell line in the presence of anti-CD8, anti- $V\delta 2$ , anti-CD3 mAbs or an unrelated mAb matched for the isotype as a control (CTR) at the E:T ratio of 5:1 (D: black columns:  $V\delta 2$  T cells from TAF co-cultures; gray columns:  $V\delta 2$  cells from CRC epithelial cell co-cultures), or in a 4 h  $^{51}\text{Cr}$  release cytotoxic assay (E, left histogram, black columns:  $V\delta 2$  T cells from TAF co-cultures; right histogram, gray columns:  $V\delta 2$  cells from CRC epithelial cell co-cultures), against untreated (white columns) or Zol-treated (black or gray columns) CaCo2 cell line at the E:T ratio of 10:1, 5:1 and 2:1. Results are expressed as percentage specific lysis calculated as described in Materials and Methods. Mean  $\pm$  SD from four experiments (left histogram) or two experiments (right histogram),  $****p < 0.0001$  or  $**p < 0.01$  Zol-treated vs. untreated CaCo2 cell line. (F) BTN3A1 localization in subcellular fractions (Cyt: cytosolic fraction, M: membrane-enriched fraction, N: nuclear fraction, Ck: cytoskeleton-enriched fraction) obtained with the Qproteome cell compartment kit from untreated or Zol-treated TAF16–027 (TAF2 in panel A). Vimentin was used as marker of the Ck fraction and GAPDH for the Cyt/M fractions.

Zol, both TAF and tissue-derived CRC cells can induce the expansion of  $V\delta 2$  effector T lymphocytes that can kill CRC cells, starting from a T cell population isolated from peripheral blood. Also,  $V\delta 2$  cytotoxic effector T cells can be derived from

tumor cell suspensions using Zol-treated peripheral blood monocytes.

All these data indicate that Zol can enable different cell types present in the CRC microenvironment (cancer cells,



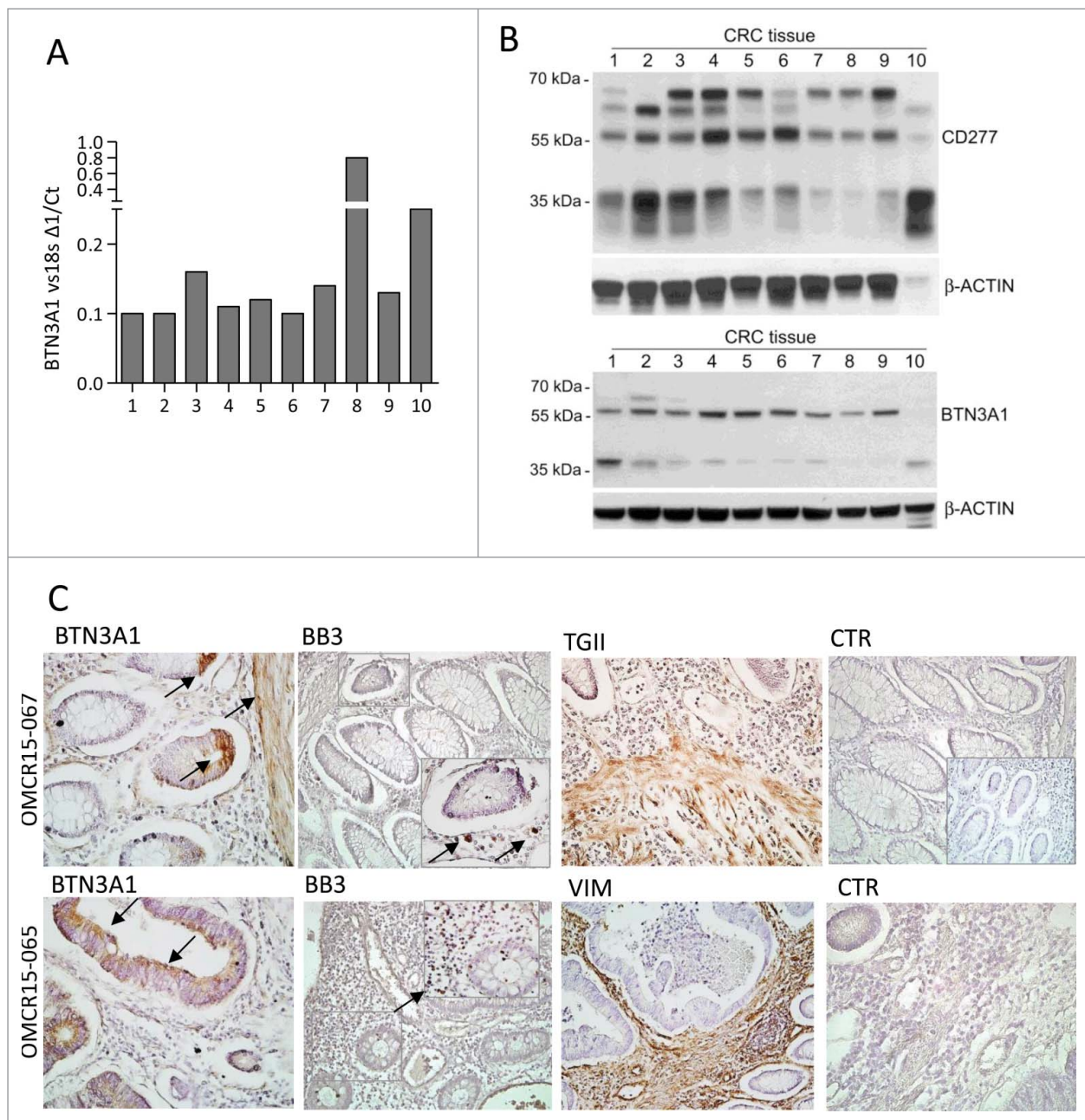


**Figure 8.** BTN3A1 expression in CRC tissue specimens. BTN3A1 expression was evaluated in CRC tissue sections by Q-RT-PCR (A), western blot (B) or immunohistochemistry (C). (A) RNA was extracted from tissue sections of 10 CRC specimens, reverse transcribed and Q-RT-PCR for BTN3A1 performed. Results are expressed as  $1/\Delta Ct$  normalized to 18s. (B) immunoblots of lysates obtained from the indicated CRC tissue specimens, as described in Materials and Methods, with the anti-CD277 mAb (upper blot) or with a rabbit polyclonal anti-BTN3A1 antiserum (lower blot).  $\beta$ -actin is shown as a loading control. (C) immunohistochemistry of two representative cases out of the 10 indicated in panels A and B, performed as described in Materials and Methods, with the indicated antibodies: polyclonal rabbit anti-BTN3A1 antiserum (arrows), anti-V $\delta$ 2 mAb (BB3, arrows in the inset), polyclonal rabbit anti-TGII antiserum, anti-vimentin mAb and a matched isotype-unrelated antibody as negative control (goat anti-rabbit antiserum in the inset of the upper CTR). Slides were counterstained with hematoxylin, coverslipped with Eukitt and analyzed under a Leica DM MB2 microscope with a charged-coupled device camera (Olympus DP70) at a 40 $\times$  enlargement, as indicated.

TAF and monocytes) to induce the expansion of antitumor  $\gamma\delta$  T lymphocytes, so that N-BPs like Zol can conceivably be proposed in therapeutic schemes of CRC. Of note, BTN3A1 could be detected by PCR in CRC specimens and by western blot as protein in cell lysates obtained from the same CRC samples. Immunohistochemistry showed that BTN3A1 can be detected on either epithelial cells or TAF

in CRC, close to areas infiltrated by V $\delta$ 2 T lymphocytes. This observation confirms that Zol can work as antitumor immune-stimulator *in vivo*; moreover, immunohistochemical analysis of BTN3A1 expression at the tumor site, together with the evaluation of BTNL2, can help to select potentially responders to Zol treatment among CRC patients.

## Methods

### CRC patients' tissue specimens

Tissue samples were obtained from 10 CRC patients undergoing therapeutic intervention at the Unit of Oncological Surgery, IRCCS-AOU San Martino-IST, Genoa, provided informed consent (the study was approved by the institutional and regional ethical committee, PR163REG2014). Samples were used for (i) preparation of cell suspensions for phenotypic and functional assays; (ii) RNA extraction for Q-RT-PCR; (iii) preparation of cell lysates for immunoblotting; and (iv) immunohistochemistry.

### Isolation of CRC cell suspension, primary tumor-associated fibroblasts and epithelial cells

CRC specimens were minced by scissors, transferred into 15 mL conical tube and digested with 2 mg/mL collagenase type I and II (Sigma-Aldrich, Darmstadt, Germany) in RPMI 1640 (Gibco, Monza, Italy) for 90 min at 37°C. Residual tissue debris were removed by soft centrifugation (300 rpm, 1 min), cells were pelleted (1,800 rpm, 10 min) and passed through a 100- $\mu$ m cell strainer (Euroclone, Milan, Italy). Cell suspensions were then purified by density gradient centrifugation (Lympholyte, Cederlane, Burlington, Ontario, Canada) and phenotypically characterized (CD3, CD14, V $\delta$ 2, CD105, EPCAM) by flow cytometry (see below). A portion of cell suspension was plated in RPMI 1640 10% fetal calf serum (FCS, Sigma), after 16 h non-adherent cells were removed and adherent cells were switched to MEM $\alpha$  (Euroclone) complete medium to obtain TAF primary cultures; after two *in vitro* passages, cells were tested for CD105 and fibroblast activation protein (FAP) expression and vimentin content and four TAF (TAF16-020, TAF16-027, TAF16-030, TAF16-035) were frozen for further experiments. The CRC15-045 and CRC13-011 epithelial cell lines were derived from a stage IIA and a stage IVB (UICC 2009) CRC, respectively, showing a strong peri- and intra-tumoral infiltration of lymphocytes. After collagenase digestion, intact crypts collected from the pellet of residual tissue debris were plated in DMEM/F12 with Hepes buffer (Euroclone), containing B27 supplement, EGF 10 ng/mL and DTT 10 nM (Sigma). The primary cell cultures initially developed as organoids, which formed small, loosely-adherent colonies after the first trypsin digestion, expressing EPCAM (not shown) and cytokeratin.

### Isolation of T cells and monocytes and co-cultures

Peripheral blood mononuclear cells (PBMC) were obtained after Ficoll-Hypaque density centrifugation of blood samples derived from healthy donors. Highly purified (> 98% pure as assessed by flow cytometry upon CD3 staining, see below) T cells were obtained from PBMC using the RosetteSep T cell Enrichment Kit (StemCell Technologies, Vancouver, Canada). Monocytes (Mo) were isolated from PBMC using the anti-CD14 mAb (MEM18, IgG1, Exbio, Prague, CZ) and EasySep custom Kit (StemCell Technologies, Inc.) according to manufacturer's instructions, with recovery of > 97% CD14 positive cells.<sup>36</sup>

The human CRC cell lines HT29, HCT15, HCT116, SW48, SW480, SW620, Colo741, Colo205, Colo320, CaCo2, LS180, WiDr, LoVo and DLD1 were obtained from the Biological Bank and Cell Factory of the IRCCS AOU San Martino IST (Genoa,

Italy) and maintained in RPMI 1640 medium supplemented with 10% FCS and 1% L-glutamine (Gibco). T cells were cultured in RPMI 1640 complete medium with or without irradiated CRC cells or TAF, or CRC15-045 cell line, at a ratio of 1:10, or Mo (Mo:T ratios from 1:10 to 1:80), untreated or exposed for 24 h to zoledronic acid (Zol 5  $\mu$ M, kindly provided as sodium salt by Novartis Pharma, Basel, Switzerland, MTA 37318); the dose was selected on the basis of the effectiveness on  $\gamma\delta$  T cells proliferation from PBMCs cultures and absence of toxic effects according to the literature and our previous data.<sup>39-41</sup> In some experiments, the CRC cell lines LS180, DLD1, HCT15 and SW620 were pre-treated for 4 h with 100  $\mu$ M or 50  $\mu$ M Zol, then washed and used for stimulation experiments.<sup>34</sup> In other experiments, 5  $\mu$ M Zol was added to the cell suspensions obtained from CRC patients' specimens. On the third day, IL-2 (4 ng/mL) was added and every 2 d complete medium supplemented with IL-2 was changed. T cells were recovered at 14 (not shown) or 20 d and V $\delta$ 2 T cell expansion was assessed by FACS analysis using the anti- $\gamma\delta$  mAb BB3 (see below).

### Immunofluorescence and cytofluorimetric analyses

Immunofluorescence was performed as described.<sup>36</sup> For the identification of  $\gamma\delta$  T cell subpopulations, we used the anti- $\gamma\delta$  mAb BB3 (IgG1).<sup>36</sup> BTN3A1 expression was checked with the anti-CD277 mAb (clone 20.1, IgG1, Affimetrix eBioscience, Hatfield, UK). Tissue-derived or cultured cell populations were also characterized with the anti-CD27 or the anti-CD45 mAb, purchased from BD Biosciences Europe (Milan, Italy), the anti-CD14 mAb (MEM18, IgG1), the anti-CD3 mAb (UCHT-1, IgG1, Ancell, Bayport, MN55003, USA), the anti-CD105 (from the producing hybridoma purchased from the American Type Culture Collection, ATCC, Manassas, VA, USA), the anti-EPCAM mAb (ab98003, IgG1, Abcam, MA, USA) or the anti-FAP mAb (F11-24, IgG1, eBioscience, San Diego, CA, USA). Negative controls were stained with APC-labeled isotype-matched irrelevant mAbs. Samples were analyzed by CyAn ADP flow cytometer (Beckman Coulter Inc., Brea, CA), gated on viable cells and/or on lymphocytes (based on FSC and SSC parameters). Results are expressed as log of mean fluorescence intensity (MFI, arbitrary units, a.u.) or percentage of positive cells.

### Cytotoxicity assay

Cytolytic activity of  $\gamma\delta$  T cells was analyzed against the various CRC cell lines at an E:T ratio of 10:1 to 2.5:1, in V-bottomed microwells, in a 4-h <sup>51</sup>Cr-release assay as described.<sup>15,16</sup> Some samples were set up after exposure of the target cell lines to Zol at 5  $\mu$ M concentration for 24 h. In some samples, the effector cells were exposed to saturating amounts (5  $\mu$ g/mL) of the anti-V $\delta$ 2 mAb at the onset of the cytotoxicity assay; an unrelated mAb, matched for the isotype (BD PharMingen, BD Italia, Milan, Italy), was used as control. Other experiments were performed using as target cells the BTN3A1-transfected SW620 or DLD1 cell lines (see below), either untreated or Zol-treated. Reverse cytotoxicity was performed using the anti-CD3 or the anti-V $\delta$ 2 or the anti-CD8 (Leu2a, IgG1, BD PharMingen) mAbs, all at 2  $\mu$ g/mL, and the Fc $\gamma$ R positive murine P815 cell line. 100  $\mu$ L of SN were measured in a  $\gamma$ -counter and the percentage of <sup>51</sup>Cr-specific release was calculated as: experimental

release (counts) - spontaneous release (counts)/maximum release (counts) - spontaneous release (counts). Maximum and spontaneous release were calculated as described.<sup>36</sup>

### **cDNA reverse transcription and quantitative real-time PCR (Q-RT-PCR)**

RNA was extracted either from cultured CRC cell lines or CRC tissue samples or cell suspensions. Paraffin-embedded sections (8- $\mu$ m thick) of the CRC patients were fixed on PEN membrane glass slides (MDS Analytical Technologies GmbH, Ismaning, Germany), dried at room temperature under a chemical safety hood for 5 min, dipped in xylene for 10 min twice for each sample, followed by a 3-step immersion in 100%/95%/75% ethanol solution. After washing in DEPC RNase-free water and staining (HistogeneActurus Italia srl, Milan, Italy), samples were dipped in 75%/95%/100% ethanol solution for 30 sec each passage followed by xylene for 5 min. Tissue sections were then dried at room temperature. RNA was extracted with the Paradise TM Reagent System (Acturus Bioscience) after incubation with proteinase K for 4 to 6 h at 56°C. A DNase treatment step was included. RNA was diluted in 50- $\mu$ L elution buffer, according to the manufacturer's protocol and quantitated by NanoDrop Spectrophotometer (ND-1000 Celbio, Euroclone) and by Qubit TM fluorometer (Invitrogen, Life Technologies Italia, Monza, Italy) using the Quant-it TM Assay Kit (Invitrogen). cDNA synthesis was performed with random hexamers by the use of the High Capacity Archive Kit (Applied Biosystems, Life Technologies). To verify quantitative RT-PCR efficiency, decreasing amounts (50 ng, 10 ng and 0.1 ng) of normal RNA were used for CT titration. For CRC cell lines, RNA was extracted with TriPure (Roche diagnostic, Milan, Italy). cDNA synthesis was performed with random primers. Primers and probes for BTN3A1 and BTNL2, were purchased by Applied Biosystem (Life Technologies Europe, Monza, Italy). Quantitative real-time PCR (Q-RT-PCR) was performed on the 7900HT FastRT-PCR system (Applied Biosystem) with the fluorescent Taqman method and normalized to 18s (Applied Biosystem). After subtracting the threshold cycle ( $C_T$ ) value for 18s from the  $C_T$  values of target genes, results were expressed as  $2^{-\Delta\Delta C_T}$  or  $\Delta C_T$  ratio vs. 18s.<sup>42</sup>

### **BTN3A1 transfection and western blot**

The pLX304-BTN3A1 plasmid (HsCD00443486, DNASU, Arizona State University) was used to overexpress BTN3A1 protein. DLD1 or SW620 cells were transfected in serum-free Opti-MEM medium (Gibco, Life Technology) with Lipofectamine 2000 (Invitrogen, Life Technology) following the manufacturer's instructions. Protein expression by western blot was analyzed from day 2 up to day 7 after transfection.<sup>42</sup> CRC cell lines were harvested and lysed with ice-cold RIPA buffer containing protease and phosphatase inhibitors. CRC tissues frozen at -80°C in 80- $\mu$ L RIPA buffer (with 1mM OV, 1mM DTT and 1:100 protease inhibitors cocktail, Sigma, P8340) were thawed on ice and minced with sharp scissors adding 100  $\mu$ L of fresh RIPA buffer to each sample. After 90 min incubation on ice, samples were potterized and centrifuged (16,000 rpm, 4°C; Eppendorf 5417-R centrifuge). Supernatants

were collected and protein content quantified by the DC protein assay (BioRad Italia, Milan, Italy). Equal amounts of protein (35  $\mu$ g/lane) were loaded under reducing or non-reducing conditions on precast 8–16% gradient gels (Thermo Fisher Scientific, Waltham, MA, USA) and then transferred to PVDF membranes (GE Healthcare, Little Chalfont, UK). After blocking, membranes were probed overnight at 4°C with the mouse monoclonal anti-CD277 (BT3.1, 20.1, Affymetrix eBioscience, recognizing the Ig-like domain of the molecule) or the rabbit polyclonal anti-BTN3A1 (NBP1-90750, Novus Biologicals, recognizing the C-terminal domain partially shared by BTN3A1 and BTN3A3) diluted according to the manufacturer's instructions. Some samples were probed with an anti-epithelial keratin 8/18 (IgG1, Cell Signaling Technology, EuroClone, Milan, Italy) or an anti-vimentin (clone V9, IgG1, Sigma) mAb. Subcellular fractionation was performed with the Q proteome cell compartment kit (Qiagen, Milan, Italy).<sup>32</sup> Enrichment of marker proteins in subcellular fractions was probed with the following antibodies: lamin B (Cell Signaling Technology), GAPDH-HRP (Novus Biologicals),  $\beta$ -tubulin (Tub2.1, Sigma) and vimentin (clone V9, Sigma). After washing, membranes were incubated for 1 h at room temperature with the relevant horseradish peroxidase (HRP)-conjugated secondary antibodies (Cell Signaling Technology), and proteins were detected by Immobilon Western Chemiluminescent HRP Substrate (Millipore, Billerica, MA, USA). Anti- $\beta$ -actin HRP-conjugated antibody (Cell Signaling) was used as a loading control.

### **Immunohistochemistry**

Paraffin-embedded samples from 10 CRC patients were analyzed for the expression *in situ* of BTN3A1, V $\delta$ 2, vimentin and TGII. Immunohistochemistry was performed on 6- $\mu$ m-thin sections, deparaffinized in xylene, and treated with Peroxoblok (Novex, Life Technologies) to quench endogenous peroxidase, followed by Ultra Blok reagent (Ultravision Detection System, Thermo Scientific BioOptica, Milan Italy). The following antibodies were added: polyclonal rabbit anti-BTN3A1 antiserum (1:100, Novus Biologicals), anti-V $\delta$ 2 mAb (BB3, 2  $\mu$ g/mL), anti-CD14 mAb (1:200, Santa Cruz Biotechnology), anti-vimentin clone V9 (1:200, Sigma), polyclonal rabbit anti-TGII antiserum (1:100, Thermo Scientific) and an isotypic-unrelated antibody was used as negative control (Dako Cytomation). Biotinylated goat anti-rabbit or goat anti-mouse antiserum (BioOptica) was then added, followed by HRP-conjugated avidin (Thermo Scientific) and the reaction developed using 3,3'-diaminobenzidine (DAB) as chromogen. Then, the slides were counterstained with hematoxylin, coverslipped with Eukitt (Bio Optica), and analyzed under a Leica DM MB2 microscope equipped with a charged coupled device camera (Olympus DP70 with a 20 $\times$  or 40 $\times$  objective).

### **HPLC negative ion electrospray ionization TOF-MS**

IPP production by the CRC cell lines SW620, LS180, DLD1, HCT15 and Colo320, either untreated or exposed to Zol, either as continuous treatment with 5  $\mu$ M for 24 h, or as pulse treatment of 50  $\mu$ M and 100  $\mu$ M for 4 h, as described in Supplementary Materials and Methods, was performed according to

Jauhiainen et al.<sup>38</sup> with modifications, as detailed in supporting information (Supplementary Materials and Methods).

The amount of IPP/DMAPP, expressed as pmol/mg protein, was evaluated by calculating the peak area of the extracted ion current (EIC  $m/z$  244.99[M-H]<sup>-</sup>), referred to a standard curve of IPP (range 0.1–15  $\mu$ M) in control cell extracts. Total protein content was determined with the DC Protein Assay (BioRad). Data are shown as IPP pmol/mg of total pmol extracted by ACN/total protein content in cell lysates after ACN extraction.

### Statistical analysis

Data are presented as mean  $\pm$  SD or SEM. Statistical analysis was performed using two-tailed Student's *t* test. The cut-off value of significance as indicated in legend to figure, was set at  $p < 0.05$  (\*),  $p < 0.01$  (\*\*),  $p < 0.001$  (\*\*\*)).

### Disclosure of potential conflict of interest

No potential conflicts of interest were disclosed.

### Acknowledgements

We thank Dr Luca Damonte and Dr Annalisa Salis (DIMES and CEBR, University of Genoa) for help in performing MS/MS experiments.

### Funding

This study was supported by research funding from the Italian Association for Cancer Research (AIRC2014, IG-15483) to AP, AIRC2015 (IG-17074) to MRZ, by the Istituto San Paolo to RB (SIME2012–0312), 5 $\times$ 1000 2012 and 5 $\times$ 1000 2013 MIUR to AP. RV and DC are recipient of a fellowship funded on the AIRC2014 (IG-15483) grant.

### ORCID

Roberta Venè  <http://orcid.org/0000-0002-2522-3716>

Roberto Benelli  <http://orcid.org/0000-0002-9769-0954>

### References

- Hayday AC. Gammadelta T cells and the lymphoid stress-surveillance response. *Immunity* 2009; 31(2):184-96; PMID:19699170; <http://dx.doi.org/10.1016/j.immuni.2009.08.006>
- Bonneville M, O'Brien RL, Born WK. Gammadelta T cell effector functions: a blend of innate programming and acquired plasticity. *Nat Rev Immunol* 2010; 10(7):467-78; PMID:20539306; <http://dx.doi.org/10.1038/nri2781>
- Poggi A, Zocchi MR.  $\gamma\delta$  T lymphocytes as a first line of immune defense: Old and new ways of antigen recognition and implications for cancer immunotherapy. *Front Immunol* 2014; 5:575; PMID:25426121; <http://dx.doi.org/10.3389/fimmu.2014.00575>. eCollection 2014; <http://www.jem.org/cgi/doi/10.1084/jem.20021500>
- Gober HJ, Kistowska M, Angman L, Jenö P, Mori L, De Libero G. Human T cell receptor gammadelta cells recognize endogenous mevalonate metabolites in tumor cells. *J Exp Med* 2003; 197(2):163-8; PMID:12538656; <http://www.jem.org/cgi/doi/10.1084/jem.20021500>
- Wang H, Sarikonda G, Puan KJ, Tanaka Y, Feng J, Giner JL, Cao R, Mönkkönen J, Oldfield E, Morita CT. Indirect stimulation of human  $V\gamma 2V\delta 2$  T cells through alterations in isoprenoid metabolism. *J Immunol* 2011; 187(10):5099-113; PMID:22013129; <http://dx.doi.org/10.4049/jimmunol.1002697>
- Kabelitz D, Kalyan S, Oberg HH, Wesch D. Human  $V\delta 2$  versus non- $V\delta 2$   $\gamma\delta$  T cells in anti-tumor immunity. *Oncoimmunology* 2013; 2(3):e23304; PMID:23802074; <http://dx.doi.org/10.4161/onci.23304>
- Corvaisier M, Moreau-Aubry A, Diez E, Bennouna J, Scotet E, Bonneville M, Jotereau F. Vgamma9 Vdelta2 T cell response to colon carcinoma cells. *J Immunol* 2005; 175(8):5481-8; PMID:16210656; <http://doi.org/10.4049/jimmunol.175.8.5481>
- Bhat J, Kabelitz D.  $\gamma\delta$ T cells and epigenetic drugs: A useful merger in cancer immunotherapy? *Oncoimmunology* 2015; 4(6):e1006088. eCollection 2015 Jun; PMID:26155411; <http://dx.doi.org/10.1080/2162402X.2015.1006088>
- Tanaka Y, Kobayashi H, Terasaki T, Toma H, Aruga A, Uchiyama T, Mizutani K, Mikami B, Morita CT, Minato N. Synthesis of pyrophosphate-containing compounds that stimulate Vgamma2 Vdelta2 T cells: application to cancer immunotherapy. *Med Chem* 2007; 3(1):85-99; PMID:17266628; <http://dx.doi.org/10.2174/157340607779317544>
- Burjanadzé M, Condomines M, Reme T, Quttet P, Latry P, Lugagne C, Romagne F, Morel Y, Rossi JF, Klein B et al. In vitro expansion of gammadelta T cells with anti-myeloma cells activity by Phosphostim and IL-2 in patients with multiple myeloma. *Br J Haematol* 2007; 139(2):206-16; PMID:17897296; <http://dx.doi.org/10.1111/j.1365-2141.2007.06754.x>
- Bennouna J, Levy V, Sicard H, Senellart H, Audrain M, Huret S, Rolland F, Bruzzoni-Giovanelli H, Rimbart M, Galéa C et al. Phase I study of bromohydrinpyrophosphate (BrHPP, IPH 1101) a Vgamma9 Vdelta2 T lymphocyte agonist in patients with solid tumors. *Cancer Immunol Immunother* 2010; 59(10):1521-30; PMID:20563721; <http://dx.doi.org/10.1007/s00262-010-0879-0>
- Capietto AH, Martinet L, Cendron D, Fruchon S, Pont F, Fournié JJ. Phosphoantigens overcome human TCRVgamma9+ gammadelta T cell immunosuppression by TGF-beta: relevance for cancer immunotherapy. *J Immunol* 2010; 184(12):6680-7; PMID:20483742; <http://dx.doi.org/10.4049/jimmunol.1000681>
- Russell RG. Bisphosphonates: the first 40 years. *Bone* 2011; 49(1):2-19; PMID:21555003; <http://dx.doi.org/10.1016/j.bone.2011.04.022>
- Das H, Wang L, Kamath A, Bukowski JF. Vgamma2Vdelta2 T-cell receptor-mediated recognition of aminobisphosphonates. *Blood* 2001; 98(5):1616-8; PMID:11520816; <http://doi.org/10.1182/blood.V98.5.1616>
- Kunzmann V, Bauer E, Feurle J, Weissinger F, Tony HP, Wilhelm M. Stimulation of gammadelta T cells by aminobisphosphonates and induction of antiplasmacyt activity in multiple myeloma. *Blood* 2000; 96(2):384-92; PMID:10887096
- Dieli F, Gebbia N, Poccia F, Caccamo N, Montesano C, Fulfaro F, Arcara C, Valerio MR, Meraviglia S, Di Sano C et al. Induction of gammadelta T-lymphocyte effector functions by bisphosphonate zoledronic acid in cancer patients in vivo. *Blood* 2003; 102(6):2310-1; PMID:12959943; <http://dx.doi.org/10.1182/blood-2003-05-1655>
- Santini D, Vespasiani Gentilucci U, Vincenzi B, Picardi A, Vasaturo F, La Cesa A, Onori N, Scarpa S, Tonini G. The antineoplastic role of bisphosphonates: from basic research to clinical evidence. *Ann Oncol* 2003; 14(10):1468-76; PMID:14504045
- Clézardin P, Fournier P, Boissier S, Peyruchaud O. In vitro and in vivo anti-tumor effects of bisphosphonates. *Curr Med Chem* 2003; 10(2):173-80; PMID:12570716; <http://dx.doi.org/10.2174/0929867033368529>
- Märten A, Lilienfeld-Toal MV, Büchler MW, Schmidt J. Zoledronic acid has direct antiproliferative and antimetastatic effect on pancreatic carcinoma cells and acts as an antigen for delta2 gamma/delta T cells. *J Immunother* 2007; 30(4):370-7; PMID:17457212; <http://dx.doi.org/10.1097/CJI.0b013e31802bff16>
- Todaro M, D'Asaro M, Caccamo N, Iovino F, Francipane MG, Meraviglia S, Orlando V, La Mendola C, Gulotta G, Salerno A et al. Efficient killing of human colon cancer stem cells by gammadelta T lymphocytes. *J Immunol* 2009; 182(11):7287-96; PMID:19454726; <http://dx.doi.org/10.4049/jimmunol.0804288>
- Lang JM, Kaikobad MR, Wallace M, Staab MJ, Horvath DL, Wilding G, Liu G, Eickhoff JC, McNeel DG, Malkovsky M. Pilot trial of interleukin-2 and zoledronic acid to augment  $\gamma\delta$  T cells as treatment for

- patients with refractory renal cell carcinoma. *Cancer Immunol Immunother* 2011; 60(10):1447-60; PMID:21647691; <http://dx.doi.org/10.1007/s00262-011-1049-8>
22. Sakamoto M, Nakajima J, Murakawa T, Fukami T, Yoshida Y, Murayama T, Takamoto S, Matsushita H, Kakimi K. Adoptive immunotherapy for advanced non-small cell lung cancer using zoledronate-expanded  $\gamma\delta$ T cells: a phase I clinical study. *J Immunother* 2011; 34(2):202-11; PMID:21304399; <http://dx.doi.org/10.1097/CJI.0b013e318207ecfb>
  23. Meraviglia S, Eberl M, Vermijlen D, Todaro M, Buccheri S, Cicero G, La Mendola C, Guggino G, D'Asaro M, Orlando V et al. In vivo manipulation of V $\gamma$ 9V $\delta$ 2 T cells with zoledronate and low-dose interleukin-2 for immunotherapy of advanced breast cancer patients. *Clin Exp Immunol* 2010; 161(2):290-7; PMID:20491785; <http://dx.doi.org/10.1111/j.1365-2249.2010.04167.x>
  24. Dieli F, Vermijlen D, Fulfaro F, Caccamo N, Meraviglia S, Cicero G, Roberts A, Buccheri S, D'Asaro M, Gebbia N et al. Targeting human gammadelta T cells with zoledronate and interleukin-2 for immunotherapy of hormone-refractory prostate cancer. *Cancer Res* 2007; 67(15):7450-7; PMID:17671215; <http://dx.doi.org/10.1158/0008-5472.CAN-07-0199>
  25. Harly C, Guillaume Y, Nedellec S, Peigné CM, Mönkkönen H, Mönkkönen J, Li J, Kuball J, Adams EJ, Netzer S et al. Key implication of CD277/butyrophilin-3 (BTN3A) in cellular stress sensing by a major human  $\gamma\delta$  T-cell subset. *Blood* 2012; 120(11):2269-79; PMID:22767497; <http://dx.doi.org/10.1182/blood-2012-05-430470>
  26. Palakodeti A, Sandstrom A, Sundaresan L, Harly C, Nedellec S, Olive D, Scotet E, Bonneville M, Adams EJ. The molecular basis for modulation of human V $\gamma$ 9V $\delta$ 2 T cell responses by CD277/butyrophilin-3 (BTN3A)-specific antibodies. *J Biol Chem* 2012; 287(39):32780-90; PMID:22846996; <http://dx.doi.org/10.1074/jbc.M112.384354>
  27. Arnett HA, Viney JL. Immune modulation by butyrophilins. *Nat Rev Immunol* 2014; 14(8):559-69; PMID:25060581; <http://dx.doi.org/10.1038/nri3715>
  28. Kabelitz D. Critical role of butyrophilin 3A1 in presenting prenyl pyrophosphate antigens to human  $\gamma\delta$ T cells. *Cell Mol Immunol* 2014; 11(2):117-9; PMID:24097034; <http://dx.doi.org/10.1038/cmi.2013.50>
  29. Vavassori S, Kumar A, Wan GS, Ramanjaneyulu GS, Cavallari M, El Daker S, Beddoe T, Theodossis A, Williams NK, Gostick E et al. Butyrophilin 3A1 binds phosphorylated antigens and stimulates human  $\gamma\delta$  T cells. *Nat Immunol* 2013; 14(9):908-16; PMID:23872678; <http://dx.doi.org/10.1038/ni.2665>
  30. Wang H, Henry O, Distefano MD, Wang YC, Rääkkönen J, Mönkkönen J, Tanaka Y, Morita CT. Butyrophilin 3A1 plays an essential role in prenyl pyrophosphate stimulation of human V $\gamma$ 2V $\delta$ 2 T cells. *J Immunol* 2013; 191(3):1029-42; PMID:23833237; <http://dx.doi.org/10.4049/jimmunol.1300658>
  31. Sandstrom A, Peigné CM, Léger A, Crooks JE, Konczak F, Gesnel MC, Breathnach R, Bonneville M, Scotet E, Adams EJ. The intracellular B30.2 domain of butyrophilin 3A1 binds phosphoantigens to mediate activation of human V $\gamma$ 9V $\delta$ 2 T cells. *Immunity* 2014; 40(4):490-500; PMID:24703779; <http://dx.doi.org/10.1016/j.immuni.2014.03.003>
  32. Rhodes DA, Chen H-C, Price AJ, Keeble AH, Davey MS, James LC, Eberl M, Trowsdale J. Activation of human  $\gamma\delta$ T cells by cytosolic interactions of BTN3A1 with soluble phosphoantigens and the cytoskeletal adaptor periplakin. *J Immunol* 2015;194(5):2390-2398; PMID:25637025; <http://dx.doi.org/10.4049/Jimmunol.1401064>
  33. Sebestyen Z, Scheper W, Vyborova A, Gu S, Rychnavska Z, Schiffler M, Cleven A, Chéneau C, van Noorden M, Peigné CM et al. RhoB mediates phosphoantigen recognition by V $\gamma$ 9V $\delta$ 2 T cell receptor. *Cell Rep* 2016; 15(9):1973-85; PMID:27210746; <http://dx.doi.org/10.1016/j.celrep.2016.04.081>
  34. Idrees ASM, Sugie T, Inoue C, Murata-Hirai K, Okamura H, Morita CT, Minato M, Toi M, Tanaka Y. Comparison of  $\gamma\delta$  T cell response- and farnesyl diphosphate synthase inhibition in tumor cells pretreated with zoledronic acid. *Cancer Sci* 2013; 104(5):536-542; PMID:23387443; <http://dx.doi.org/10.1111/cas.12124>
  35. Dieli F, Poccia F, Lipp M, Sireci G, Caccamo N, Di Sano C, Salerno A. Differentiation of effector/memory V $\delta$ 2 T cells and migratory routes in lymph nodes or inflammatory sites. *J Exp Med* 2003; 198(3):391-397; PMID:12900516; <http://dx.doi.org/10.1084/jem.20030235>
  36. Musso A, Catellani S, Canevali P, Tavella S, Venè R, Boero S, Pierri I, Gobbi M, Kunkl A, Ravetti JL et al. Aminobisphosphonate prevent the inhibitory effect exerted by lymph node stromal cells on anti-tumor V $\delta$ 2 T lymphocytes in non-Hodgkin lymphomas. *Haematologica* 2014; 99(1):131-9; PMID:24162786; <http://dx.doi.org/10.3324/haematol.2013.097311>
  37. Arnett HA, Escobar SS, Gonzalez-Suarez E, Budelsky AL, Steffen LA, Boiani N, Zhang M, Siu G, Brewer AW, Viney JL. BTN2L2, a butyrophilin/B7-like molecule, is a negative costimulatory molecule modulated in intestinal inflammation. *J Immunol* 2007; 178(3):1523-33; PMID:17237401; <http://doi.org/10.4049/jimmunol.178.3.1523>
  38. Jauhainen M, Monkkonen H, Raikkonen J, Monkkonen J, Auriola S. Analysis of endogenous ATP analogs and mevalonate pathway metabolites in cancer cell cultures using liquid chromatography-electrospray ionization mass spectrometry. *J Chromatogr B Analyt Technol Biomed Life Sci* 2009; 877(27):2967-75; PMID:19665949; <http://dx.doi.org/10.1016/j.jchromb.2009.07.010>
  39. Bouet-Toussaint F, Cabillic F, Toutirais O, Le Gallo M, Thomas de la Pintièrre C, Genetet N, Meunier B, Dupont-Bierre E, Boudjema K et al. V $\gamma$ 9V $\delta$ 2 T cell-mediated recognition of human solid tumor. Potential for immunotherapy of hepatocellular and colorectal carcinomas. *Cancer Immunol Immunother* 2008; 57(4):531-539; PMID:17764010; <http://dx.doi.org/10.1007/s00262-007-0391-3>
  40. Musso A, Zocchi MR, Poggi A. Relevance of the mevalonate biosynthetic pathway in the regulation of bone marrow mesenchymal stromal cell-mediated effects on T-cell proliferation and B-cell survival. *Haematologica* 2011; 96(1):16-23; PMID:20884711; <http://dx.doi.org/10.3324/haematol.2010.031633>
  41. Fiore F, Castella B, Nuschak B, Bertieri R, Mariani S, Bruno B, Pantaleoni F, Foglietta M, Boccadoro M, Massaia M. Enhanced ability of dendritic cells to stimulate innate and adaptive immunity on short-term incubation with zoledronic acid. *Blood* 2007; 110(3):921-7; PMID:17403919; <http://dx.doi.org/10.1182/blood-2006-09-044321>
  42. Zocchi MR, Camodeca C, Nuti E, Rossello A, Venè R, Tosetti F, Dapino I, Costa D, Musso A, Poggi A. ADAM10 new selective inhibitors reduce NKG2D ligand release sensitizing Hodgkin lymphoma cells to NKG2D-mediated killing. *Oncoimmunol* 2016; 5:5, e1123367; PMID:27467923; <http://dx.doi.org/10.1080/2162402X.2015.1123367>